Mesopotamian Journal of Civil Engineering
Vol.2026, **pp**. 125–138
DOI: https://doi.org/10.58496/MJCE/2026/011; ISSN: 3006-1148
https://mesopotamian.press/journals/index.php/MJCE

Research Article

Explicit models for the geotechnical and structural assessment of pavement using falling weight deflectometer results and core samples

Saif Alzabeebee[1,2, *], Suraparb Keawsawasvong[3]

[1] *Department of Roads and Transport Engineering, College of Engineering, University of Al-Qadisiyah, Iraq.*

[2] *College of Engineering, University of Warith Al-Anbiyaa, Karbala, Iraq.*

[3] *Department of Civil Engineering, Thammasat School of Engineering, Thammasat University, Thailand.*

ARTICLE INFO

Article History

Received 06 Sep 2026
Revised 20 Oct 2026
Accepted 21 Nov 2026
Published 23 Nov 2026

Keywords

Falling weight deflectometer
Equivalent thickness
Equivalent stiffness
Geotechnical assessment
Pavement

ABSTRACT

This study develops new models to predict equivalent thickness and stiffness for the geotechnical and structural assessment of a pavement section using multi-objective evolutionary polynomial regression analysis. The database has been developed based on a validated three-dimensional finite element model. The finite element model has been validated against field results of a falling weight deflectometer test. The accuracy of the new models has been assessed using the mean absolute error (MAE), mean, coefficient of correlation (R), and cumulative frequency of error. The developed equation of the equivalent thickness of the pavement section scored values of MAE, mean, and R of 97, 1.00, and 0.86, respectively, for the training set and 100, 1.00, and 0.84, respectively, for the testing set. Furthermore, the equation developed to predict the equivalent stiffness of the pavement section scored values of MAE, mean, and R of 15612, 1.01, and 0.94, respectively, for the training set and 18078, 1.00, and 0.94, respectively, for the testing set. Also, both models have been noted to retain high frequency at low error, which further confirms the accuracy. Thus, these models could be of significant help to engineers working on pavement design and quality control.

1. INTRODUCTION

The equivalent pavement section thickness methodology is a well-established method that provides a straightforward simplification in the analysis and assessment of the geotechnical and structural capacity of the pavement [1]. This method converts the multilayers of the pavement into a single layer with equivalent thickness and equivalent stiffness. The benefit of this method is not only in the design but also in the assessment of the actual structural condition of a pavement with the availability of the falling weight deflectometer (FWD) test, as the obtained thickness and stiffness could be easily compared with the design values for the pavement. However, the main challenge in such a method is the lack of available equations to predict the equivalent thickness and stiffness of the layer, which is due to the fact that past studies focused solely on using the results of the FWD test to develop black box models to predict the pavement properties using the results of the FWD test [2-8], as will be explained in the next paragraph.

Sharma and Das [2] developed black-box algorithms to predict the asphalt layer stiffness, granular layer stiffness, subgrade layer stiffness, and distance to the rigid layer using artificial neural networks and the results of FWD tests. They found that the lowest error is found for the algorithm developed to predict the subgrade stiffness. In addition, they compared the prediction of the developed algorithms with the prediction of available back-calculation software packages (EVERCALC and ExPaS) and found that the developed algorithms outperformed the aforementioned software packages. Saltan et al. [3] utilized an artificial neural network to develop a black box model to back-calculate the stiffness, thickness, and Poisson ratio of the asphalt layer using the results of a falling weight deflectometer test. The database utilized in the study was developed by the author using a finite element software package called SDUFEM. Terzi et al. [4] developed a black box model to predict the pavement layer thickness using the results of the falling weight deflectometer. The database developed by Saltan et al. [3] was utilized in this study. Phulsawat et al. [5] developed black box models to predict the stiffness of asphalt, base, subbase, and subgrade of a pavement section. The algorithms utilized in the development of the models were the artificial neural network (ANN) and the random forest regression (RFR), while the database was developed using the exact stiffness method. Ma et al. [6] used four different machine learning methods (support vector regression, random forest regression,

*Corresponding author. Email: saif.alzabeebee@qu.edu.iq

eXtreme gradient boosting, and backpropagation neural network) to develop black box models to estimate the stiffness of asphalt, subbase, and subgrade stiffness. They found that the backpropagation neural network algorithms provided more accurate results than the other methods for the stiffness of the asphalt and subbase layer. In addition, they found that the eXtreme Gradient Boosting algorithm exhibited the best prediction for subgrade stiffness. Wang and Zhao [7] also developed black-box algorithms to estimate the stiffness of the pavement layers using different data-driven techniques. Gajewski et al. [8] examined the capabilities of the XGBoost ML regression model in the estimation of pavement parameters.

It is evident from the literature review discussed in the previous section that past studies focused on the development of black box models to predict the stiffness of pavement layers using the results of FWD. However, it is clear that the back box model cannot be tested or utilized by others, and thus, these models did not solve the issue of the time and skills and cost of back calculation techniques required for pavement assessment. Hence, an effort is made in this study to provide alternative models that enable the pavement assessment using results of FWD and core samples. These models enable the prediction of the equivalent thickness and stiffness of the pavement section. The next section briefly explains the meaning of the equivalent thickness and stiffness. It is also important to state that the use of an equivalent single-layer representation is based on the well-established Odemark method. This approach simplifies the analysis of multilayer pavement systems by transforming their properties into equivalent parameters, thereby reducing computational complexity. The objective of the developed models is not to reproduce all aspects of interlayer interactions but to provide a practical and efficient means of estimating equivalent pavement thickness and stiffness for pavement evaluation. Furthermore, as will be explained throughout the paper, the developed models demonstrated good statistical performance, supporting their potential as a convenient alternative to conventional FWD back-calculation procedures, which typically require specialized expertise, computational tools, and considerable time. The authors acknowledge the simplifying assumptions inherent in the equivalent-layer approach; however, these assumptions are consistent with the intended scope and practical application of the proposed model.

2. EQUIVALENT THICKNESS and STIFFNESS

The method of equivalent thickness is widely used in pavement engineering due to its simplicity and evidence from industry of its effectiveness [1]. This method changes the whole pavement section into an equivalent section (i.e., one section with equivalent thickness and stiffness). Although the thickness and stiffness are not real material properties, these assumptions simplify the complex interaction of the pavement layers and change the whole section into one layer that could be utilized for a quick and convenient check for the quality of the pavement. Note that this method is easier compared to back-calculation, as the latter requires specialized software, several iterations, and a skilled person to do the work. The equivalent pavement section thickness (h_e) could be predicted based on the Odemark method, and it is in Equation 1 [9, 10]. In addition, the equivalent pavement section stiffness (E_c) could be calculated using Equation 2, which has been obtained from rearranging Equation 1.

$$h_e = \sum C h_i \left(\frac{E_i}{E_{sg}}\right)^{1/3} \quad (1)$$

$$E_c = E_{sg} \left(\frac{h_e}{H}\right)^3 \quad (2)$$

Where, C is a constant which ranges from 0.8 to 0.9, and it is taken equal to 0.85 in this study; hi is the layer thickness, E_i is the layer stiffness, E_{sg} is the subgrade stiffness, H is the thickness of the pavement section above the subgrade.

3. CONTRIBUTION OF THE STUDY

The idea of this paper is to use a defined database to enable the prediction of the equivalent thickness and stiffness using inputs that could be readily obtained from a routine FWD test and a core sample. These inputs are the pavement deflection under the point load (do), the deformation of the pavement at a distance of 0.3 m ($d30$), the surface curvature index (SCI), asphalt layer stiffness ($E_{asphalt}$), and asphalt layer thickness ($t_{asphalt}$). Note that do and $d30$ are obtained from the FWD test, while the SCI is the difference between do and $d30$. In addition, the asphalt layer thickness and stiffness could be simply obtained using a core sample. Thus, the novelty of this work is to provide straightforward models that could be easily utilized to find the equivalent thickness and stiffness of a pavement section from basic parameters that could be obtained from a routine FWD test. These models have the potential to replace time-consuming back-calculation analysis.

4. METHODOLOGY

The methodology involves using a validated finite element model of a falling weight deflectometer to generate a database that enables the development of new explicit models. Section 4.1 discusses the finite element model development. In addition, Section 4.2 details the results of the validation. Section 4.3 briefly explains the methodology used to develop the models, and finally, Section 4.4. explains the methodology of the accuracy assessment of the developed models.

4.1 Finite element model details

Plaxis 3D has been used to develop the finite element model utilized in this study. The length, width, and depth of the finite element model were considered equal to 20, 20, and 10 m, respectively. These dimensions have been selected after a sensitivity study to ensure that the model size does not affect the results. In addition, 10-noded elements have been used to model the soil and the steel plate of the FWD test, as these are the only elements available in Plaxis 3D. The nodes at the sides of the model have been restrained against movement in horizontal directions, while the nodes at the bottom of the model have been fixed to prevent movement in all of the directions. These boundaries are also illustrated in Figure 1. Furthermore, viscous boundary conditions have been installed at the sides and bottom of the models in the dynamic analysis to prevent wave reflection, which could affect the results. The viscous boundary conditions in Plaxis 3D are formulated based on the methodology of Lysmer and Kuhlmeyer [11], where they proposed to use dashpots in the normal and tangential directions to dissipate the incoming stresses during the dynamic analysis as shown in Equation 3 and 4.

$$\sigma_n = -C_1 \times \rho \times V_p \times v_n \quad (3)$$

$$\tau_n = -C_2 \times \rho \times V_s \times v_s \quad (4)$$

Where, σ_n is the normal viscous stress applied at the boundary to absorb outgoing waves, C_1 is the relaxation coefficient for normal stress absorption associated with compressional waves, ρ is the density of the material adjacent to the boundary, V_p is the compression propagation velocity of the material adjacent to the boundary, v_n is the particle velocity component normal to the boundary, τ_n is the tangential viscous stress applied at the boundary, C_2 is the relaxation coefficient for shear stress absorption associated with shear waves, V_s is the shear wave velocity of the material adjacent to the boundary, and v_s is the velocity component tangential to the boundary. It is important to mention that the values of C_1 and C_2 are considered equal to 1.0 as suggested in the Plaxis manual for Problems of surface vibration [12].

The falling weight deflectometer has been modeled as a uniformly distributed load applied directly on the steel plate of the test as shown in Figure 1. The applied load has been fed to Plaxis as an impact load function to allow realistic modeling of the test. The dynamic time step has been taken equal to 0.005 sec. This time step has been decided based on the validation problem, which will be demonstrated in Section 4.2.

The linear elastic model has been used to model the subgrade, subbase, asphalt layer, and steel plate of the falling weight deflectometer. This model has been used, as past studies demonstrated that this model produces reasonable results in the replication of the FWD test [13-17], which is justifiable as the pavement's FWD test load is within the linear elastic range. Also, the validity of this model in replicating the results of the FWD test will be demonstrated in the validation section (Section 4.2).

The mesh has been refined at the entire surface to ensure accurate results since the load is applied at the surface. An example of the utilized mesh is shown in Figure 1. Also, the analysis has been carried out in two steps. The first step is the static step, which involved the calculation of the initial stress of the pavement section (asphalt layer, subbase, and subgrade), while the second step involved the dynamic analysis of the FWD test.

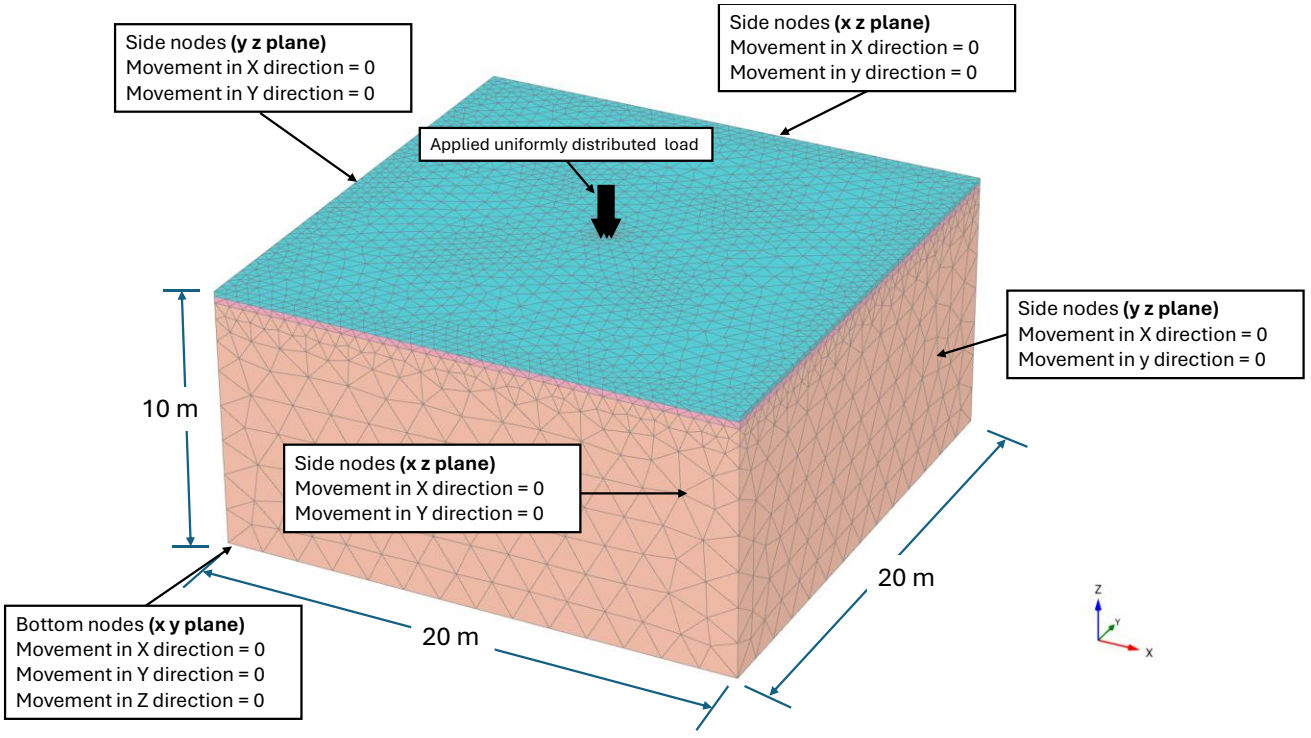


Fig. 1. The finite element mesh of the problem

4.2 Finite element model validation with field results

The validation involved comparing the results of the finite element model of the present study with well-documented results of the FWD test to check the accuracy of the finite element model and to utilize the results as a benchmark to develop the database that would be used in the data-driven modelling of the new models. For this purpose, a thorough literature review has been carried out to find a field study that reports the full details of the falling weight deflectometer test and the material properties of the pavement layers to enable correct replication of the problem without any assumption being made in the modeling stage. As a result of this review, the authors found the paper of Loizos and Scarpas [17], who reported field results of falling weight deflectometer tests for two pavement sections in Greece. Both pavement sections comprised an asphalt layer, a subbase layer, and a subgrade layer. The average thickness of the asphalt and subbase layers was equal to 0.19 and 0.45 m, respectively, for the first pavement section (referred to as K1 from this point forward). The second section (K8) has values of 0.195 and 0.475 m for the average thickness of the asphalt layer and the subbase layer, respectively.

In addition, the impact load of the falling weight deflectometer was applied in the field test using a plate with a diameter of 0.3 m for both sections. The impact load applied in the test of both sections has a peak value of 50 kN, with the dynamic function being reported by Loizos and Scarpas [17] and is shown in Figure 2. In addition, the stiffness of the pavement layers for both sections are reported in the paper of Loizos and Scarpas [17], who found them using back-calculation analysis utilizing the MODULUS software package. These values are shown in Table 1.

The same problem has been modeled using the finite element model of the present study (i.e., in Plaxis 3D). The utilized model dimensions, mesh refinement, element types, time step, and steps of analysis were similar to those discussed in Section 4.1. In addition, the plate diameter of the FWD test is considered equal to 0.3 m, similar to the field test. More importantly, the impact load reported in Figure 2 is fed to the Plaxis 3D model using the table function to allow accurate replication of the test.

Figure 3 shows the relationship of settlement below the impact point (maximum value) and time for both sections as an example of the output of the developed numerical models. It is clear that the shape of the settlement-time relationship is similar to the function of the applied impact point, which is expected. In addition, Figures 4 and Figure 5 compare the field results reported by Loizos and Scarpas [17] and the finite element model predictions of the relationship of the maximum settlement induced due to the impact load and the distance from the impact load (plate) for K1 and K8 sections, respectively.

It is evident from Figures 4 and 5 that the finite element model of the present study predicts the same trend of settlement over the distance from the impact point. In addition, both models provide a good prediction of the maximum settlement (overpredicted by about 1% and 8%, respectively). However, there are some discrepancies as the distance from the impact point increases, which may be attributed to the simplified linear-elastic subgrade and the idealized boundary conditions.

Nonetheless, both models provide meaningful results, with mean absolute errors of 0.014 and 0.016 mm for Figures 4 and 5, respectively. Based on these comparisons, the model of the present study captures the trend of the relationship well and gives reasonable accuracy. Hence, the model developed in this study could be utilized to generate a robust database.

TABLE I. MATERIAL PROPERTIES REPORTED BY LOIZOS AND SCARPAS [17] FOR K1 AND K8 SECTIONS

Pavement layer	Stiffness (kPa)	
	K1 section	K8 section
Asphalt Layer	4,578,000	4,473,000
Subbase layer	196,700	123,900
Subgrade Layer	162,000	396,900

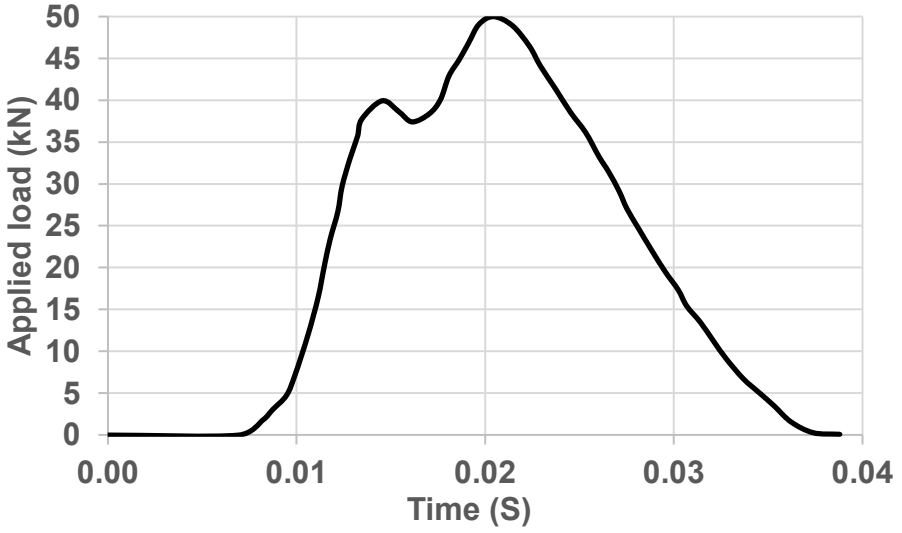


Fig. 2. The dynamic load applied in the FWD test for sections K1 and K8 as reported by Loizos and Scarpas [17]

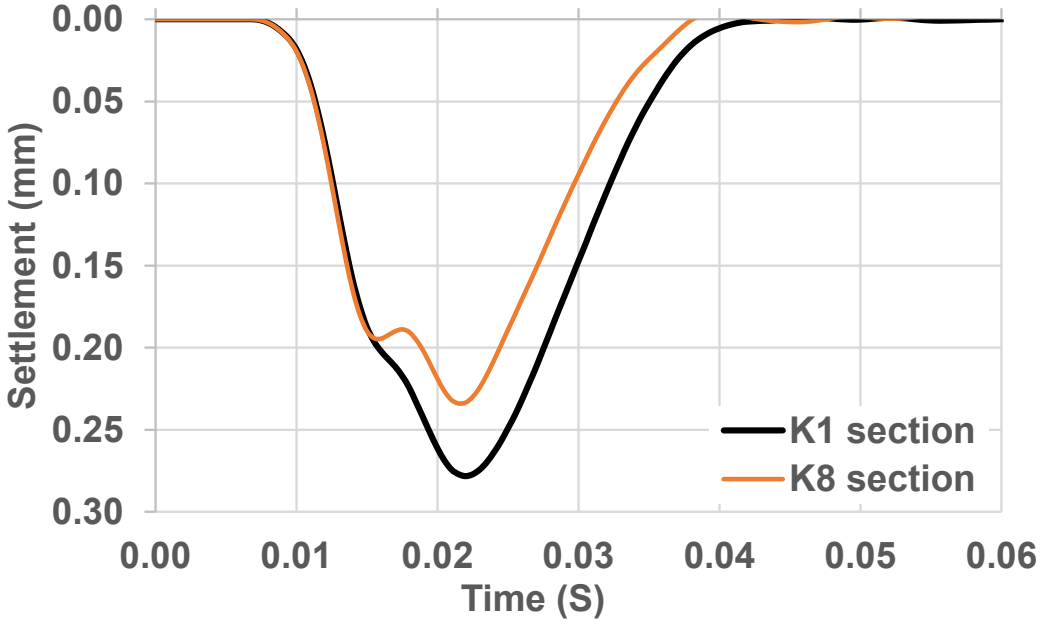


Fig. 3. The obtained settlement-time relationship below the impact point for Sections K1 and K8

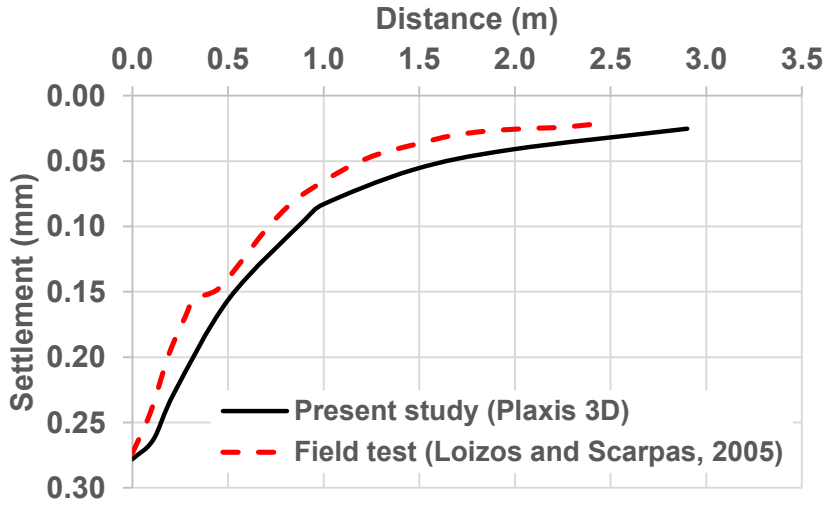


Fig. 4. Results of the validation of the finite element model of the present study for section K1

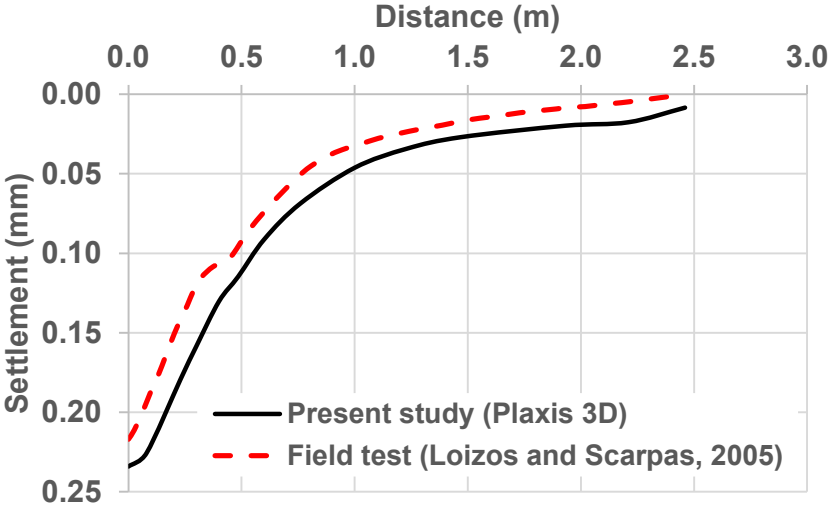


Fig. 5. Results of the validation of the finite element model of the present study for section K8

4.3 Method used to develop the model

The method utilized to develop the models is the multi-objective evolutionary polynomial regression analysis (MOGA-EPR). This method was developed by Giustolisi and Savic [18]. MOGA-EPR is a hybrid data-driven technique that combines a genetic algorithm (GA) with the least-squares method to generate symbolic, polynomial-type expressions. The structure of the model in this method is searched by the GA, and the numerical coefficients are estimated by linear least squares. The general form of the EPR-MOGA model is shown in Equation 5.

$$y_{predicted} = a_0 + \Sigma_j\, a_j \cdot (X_1)^{ES(j,1)} \cdot (X_2)^{ES(j,2)} \cdots (X_k)^{ES(j,k)} \cdot f(\cdot), \quad j = 1, \ldots, m \tag{5}$$

Where, $y_{predicted}$ is the predicted output, a_0 is the bias (constant) term, a_j are the coefficients estimated by least squares, m is the number of terms, k is the number of input variables, Xi are the input variables, ES(j,i) is the exponent of input i in term j, selected by the GA from a user-defined set of candidate exponents, and f(·) is an optional inner function (e.g., none, exponential, logarithmic, or hyperbolic tangent).

In the multi-objective formulation, the GA searches simultaneously for models that (i) maximize the fit to the data, measured by the coefficient of determination, and (ii) minimize model complexity, measured by the number of terms (and, where used, the number of inputs). The resulting set of non-dominated models forms the Pareto front, from which the final expression is selected.

The MOGA-EPR was selected in this study because the objective of this research was not only to achieve accurate prediction but also to develop an explicit mathematical relationship that can be readily implemented in engineering practice. Unlike many conventional machine-learning models, which may require specialized software or retain complex internal structures, MOGA-EPR produces explicit mathematical models while simultaneously allowing prediction accuracy and model complexity to be considered during model selection. The resulting models can therefore be directly implemented in a spreadsheet or simple computational tool, facilitating their use by pavement engineers without requiring access to the original machine-learning algorithm [19-21].

4.4 Methodology used to examine accuracy of the developed model

The accuracy of the prediction of each model has been checked using well-known accuracy measures. These are the mean absolute error (MAE), the mean, and the coefficient of correlation (R) [5,21,22]. The equations used to calculate the aforementioned measures are shown in Equations 6-8 [21,22]. Note that the MAE has been used because it is less affected by the outliers; thus, it provides the representative measure of the performance of prediction [22]. In addition, the mean has been utilized, as it shows the overall performance of the model in terms of overprediction or underprediction, where a value more than 1 indicates an overall overprediction, while a value less than 1 indicates a tendency of underprediction [21]. Also, the cumulative frequency of error has also been checked to check the cumulative error level of the developed models [23].

$$MAE = \frac{1}{n}\sum_{i=1}^{n}\left|y_{input} - y_{predicted}\right| \tag{6}$$

$$\text{Mean} = \frac{1}{n}\sum_{i=1}^{n}\frac{y_{input}}{y_{predicted}} \tag{7}$$

$$R = \frac{\sum_{i=1}^{n}\left[\left(y_{input} - y_{input\ mean}\right) \times \left(y_{predicted} - y_{predicted\ mean}\right)\right]}{\sqrt{\left\{\left[\sum_{i=1}^{n}\left(y_{input} - y_{input\ mean}\right)^2\right] \times \left[\sum_{i=1}^{n}\left(y_{predicted} - y_{predicted\ mean}\right)^2\right]\right\}}} \tag{8}$$

Where, y_{input} is the input value of the dependent variable (i.e., measured value, which is equivalent to thickness or stiffness obtained based on finite element results), $y_{predicted}$ is the predicted value of the dependent variable using the developed models, n is the number of cases considered in the error assessment, $y_{input\ mean}$ is the mean of the dependent variable, and $y_{predicted\ mean}$ is the mean of the predicted value of the dependent variable.

5. DATABASE

The database, as stated earlier, has been generated using the validated finite element model of this study. Detailed analysis was conducted for different values of asphalt layer thickness ($t_{asphalt}$), subbase layer thickness ($t_{subbase}$), asphalt layer stiffness ($E_{asphalt}$), subbase layer stiffness ($E_{subbase}$), and subgrade layer stiffness ($E_{subgrade}$). The adopted values utilized for the aforementioned parameters are shown in Table 2.

It is important to state that the range adopted for the pavement section variables has been collected from the literature to reflect vast scenarios and so that the predictive model becomes as general as possible. It is clear in Table 2 that the considered asphalt layer thicknesses are 50 and 100 mm. This consideration has been made, as these values are within the range that is commonly adopted for pavement [24, 25]. Also, Table 2 shows that the considered range for the subbase thickness is between 150 and 450 mm, which covers the representative range of subbase thickness reported and adopted in pavement design and experimental studies [26,27]. In addition, the table illustrates that the adopted range for the asphalt layer stiffness is very wide and ranges between 48,260 and 13,789,490 kPa. This wide range has been considered because asphalt is strongly affected by the temperature and loading frequency, and the selected range considers the wide variations reported in literature for asphalt stiffness with different temperature and frequency values [e.g., 28,29]. Furthermore, the considered range of stiffness of the subbase layer is between 68,940 and 344,740 kPa to cover the weak subbase layer and the expected range of subbase layer stiffness commonly adopted in pavement design and analysis [30,31]. In addition, the subgrade stiffness was varied from 34,470 to 162,400 kPa (34.5–162.4 MPa), covering a representative range of subgrade modulus values reported for different soil types and moisture conditions [32]. Thus, the total number of scenarios considered in this study are 384 scenarios, which is also demonstrated in Table 2.

It is worthy to mention that the total model depth was kept constant at 10 m in all runs. The thicknesses of the asphalt layer (up to 0.10 m) and the subbase layer (up to 0.45 m) were varied according to Table 2, and the subgrade thickness was adjusted accordingly so that the total depth remained 10 m (i.e., $t_{subgrade} = 10 - t_{asphalt} - t_{subbase}$). Therefore, the subgrade thickness ($t_{subgrade}$) ranged from about 9.45 m to 9.8 m. In addition, it should be emphasized that for each run (scenario), the values of d_o and d_{30} has been obtained, and the SCI has been calculated as the difference between d_o and d_{30}. The obtained values and the input values were then utilized to calculate the equivalent thickness (h_e) and the equivalent stiffness (E_c) using Equations 1 and 2. Note that each finite element run took about 30 minutes.

Table 3 shows a representative sample of the database used in the development of the models. Furthermore, Table 4 shows the basic statistical indicators for each independent and dependent variable. In addition, the whole generated database is uploaded as a supplementary material.

TABLE II. THE VALUES ADOPTED IN THE FINITE ELEMENT MODEL ANALYSIS AND TOTAL NUMBER OF ANALYSES

Parameter	Number of levels	Values	Reference
$t_{asphalt}$ (mm)	2	50 and 100	Selezneva et al. [24] and Nogima et al. [25]
$t_{subbase}$ (mm)	4	150, 260, 300, and 450	Christopher et al. [26] and the Ministry of Transport of the People's Republic of China [27]
$E_{asphalt}$ (kPa)	4	48260, 4570000, 6918875, and 13789490	Li et al. [28] and Nguyen et al. [29]
$E_{subbase}$ (kPa)	4	68940, 169700, 206840, and 344740	Yi et al. [30] and Chua et al. [31]
$E_{subgrade}$ (kPa)	3	34470, 98000, and 162400	Pierce et al. [32]
Total analyses	$2 \times 4 \times 4 \times 4 \times 3 = 384$		

TABLE III. EXAMPLE OF THE DATABASE USED IN THE DEVELOPMENT OF THE NEW EQUATION

No.	d_o (mm)	d_{30} (mm)	SCI (mm)	$t_{asphalt}$ (mm)	$E_{asphalt}$ (kPa)	h_e (mm)	E_c (kPa)
1	0.6432	0.5032	0.14	100	4570000	983	84695
2	0.6776	0.4585	0.22	100	6918875	465	182164
3	1.3030	0.6537	0.65	50	6918875	516	101104
4	0.3215	0.2271	0.09	100	13789490	537	349135
5	0.4028	0.2128	0.19	50	13789490	678	220340
6	0.6286	0.2853	0.34	50	6918875	537	174282
7	1.3340	0.8969	0.44	50	13789490	545	93904
8	0.4167	0.2665	0.15	100	6918875	521	235090
9	0.6733	0.2789	0.39	50	6918875	278	225588
10	0.2905	0.2083	0.08	100	13789490	701	284738
11	0.4579	0.3047	0.15	100	6918875	811	144440
12	0.7634	0.6032	0.16	100	6918875	899	86106
13	0.2972	0.2118	0.09	100	13789490	658	296663
14	0.3468	0.2249	0.12	100	6918875	581	262050
15	3.3630	1.2040	2.16	100	48260	312	43017
16	0.6732	0.2807	0.39	50	4570000	406	188236
17	0.7411	0.3546	0.39	50	4570000	612	120010
18	2.1410	0.3261	1.81	100	48260	296	133655
19	0.6966	0.3981	0.30	50	13789490	486	153777
20	0.3922	0.2426	0.15	100	6918875	711	210083

TABLE IV. BASIC STATISTICAL PARAMETERS OF THE DEPENDENTS AND INDEPENDENT VARIABLES OF THE DATABASE

Statistical parameter	d_o (mm)	d_{30} (mm)	SCI (mm)	$t_{asphalt}$ (mm)	$E_{asphalt}$ (kPa)	h_e (mm)	E_c (kPa)
Min value	0.27	0.18	0.08	50	48260	124	35260
Max value	4.11	1.31	2.81	100	13789490	1450	349135
Standard deviation	0.84	0.25	0.71	25	4970058	239	66378
Mean	1.16	0.50	0.66	75	6331656.25	566	137639

6. THE NEW MODELS

The first step in the development of the models was the separation of the database into training and testing. The training data comprises 80% of the database, while the remaining data are used to test the model. These ratios have been decided based on past studies on the use of machine learning in the development of new models [e.g., 3,5]. The training means that the data will be used to train the model to accurately capture the factors affecting the prediction so that accuracy is ensured. On the other hand, the testing data are used to examine the prediction accuracy of the model in the prediction for scenarios that have not been utilized to train the model. The data separation has been carried out using the random shuffle function in Excel with careful checks to ensure that the range of the testing data is within that of the training data. This condition is important to avoid extrapolation of the model in the testing stage [5,33,34]. Tables 5 and 6 show the basic statistical indicators of the two sets, which demonstrates that the aforementioned condition has been achieved.

The developed training and testing sets have been fed to the EPR-MOGA algorithm to develop the new models of the he and Ec. The EPR-MOGA runs were carried out using the EPR-MOGA XL software package. The settings used are shown in Table 7. The number of terms was searched between 1 and 8, and the candidate exponents were as stated in Table 7. The model for each output was selected from the Pareto front as the equation that gave low error and high accuracy with a small number of terms, and the accuracy was then checked on the testing set. Several searches for the best mathematical model that provides the lower error and higher accuracy and the most accurate models found are shown in Equations 9 and 10 for the prediction of the he and Ec, respectively.

$$he = \frac{16425.2843 \times \sqrt{d_{30}} \times {t_{asphalt}}^2}{\sqrt{\text{SCI}} \times {d_o}^2 \times E_{asphalt}} - \frac{14.3051 \times \sqrt{t_{asphalt}}}{\sqrt{d_{30}}} - \frac{0.0054675 \times \sqrt{t_{asphalt}} \times \sqrt{E_{asphalt}}}{\sqrt{\text{SCI}}} + \frac{2377.6794 \times \sqrt{d_{30}}}{\text{SCI} \times \sqrt{t_{asphalt}}} + 228.5848 \quad (9)$$

$$Ec = -\frac{60.38 \times {t_{asphalt}}^2}{\sqrt{E_{asphalt}} \times {d_o}^2 \times {d_{30}}^2} + \frac{898899632.6101 \times \sqrt{\text{SCI}}}{\sqrt{d_{30}} \times \sqrt{E_{asphalt}} \times d_o \times t_{asphalt}} + \frac{1.1243 \times \text{SCI} \times t_{asphalt} \times \sqrt{E_{asphalt}}}{\sqrt{d_o} \times d_{30}} - \frac{3.7602 \times d_o \times \text{SCI} \times E_{asphalt}}{{d_{30}}^2 \times {t_{asphalt}}^2} - 4277.0736 \quad (10)$$

Figures 6 and 7 compare the predicted values of he (Equation 9) and Ec (Equation 10), respectively, against the input values, along with the no-error line and the ±20% error limits for training and testing datasets. It is evident that the prediction of both variables is reasonable, as most points are near the no-error line. In addition, Tables 8 and 9 show the scored MAE, mean, and R for both data sets for Equations 9 and 10, respectively. The tables show that both models scored low error, optimum mean value, and high R value. This again demonstrates the prediction accuracy. Finally, Figure 8 presents the cumulative frequency of the prediction error obtained using the developed models. Both models demonstrate good predictive performance, with a high proportion of the predictions falling within relatively low error levels. However, Equation 10 consistently exhibits a lower prediction error at a given cumulative frequency compared with Equation 9, indicating better overall predictive performance. For example, at an error level of 20%, the cumulative frequency is approximately 60% for Equation 9, whereas it reaches approximately 78% for Equation 10. This indicates that approximately 78% of the predictions obtained from Equation 10 have errors of 20% or less, compared with approximately 60% for Equation 9.

In conclusion, it is evident both models scored reasonably well in terms of accuracy checks, and thus, these models could be helpful for pavement engineers working on pavement quality control checks.

TABLE V. BASIC STATISTICAL PARAMETERS OF THE DEPENDENTS AND INDEPENDENT VARIABLES OF THE TRAINING SET

Statistical parameter	d_o (mm)	d_{30} (mm)	SCI (mm)	$t_{asphalt}$ (mm)	$E_{asphalt}$ (kPa)	h_e (mm)	E_c (kPa)
Min value	0.27	0.18	0.08	50	48260	124	35260
Max value	4.11	1.31	2.81	100	13789490	1450	349135
Standard deviation	0.84	0.25	0.71	25	4953804	243	65542
Mean	1.17	0.50	0.67	74	6350846	561	135895

TABLE VI. BASIC STATISTICAL PARAMETERS OF THE DEPENDENTS AND INDEPENDENT VARIABLES OF THE TESTING SET

Statistical parameter	d_o (mm)	d_{30} (mm)	SCI (mm)	$t_{asphalt}$ (mm)	$E_{asphalt}$ (kPa)	h_e (mm)	E_c (kPa)
Min value	0.31	0.19	0.08	50	48260	187	35881
Max value	3.81	1.22	2.65	100	13789490	1322	326737
Standard deviation	0.85	0.25	0.70	25	5064977	226	69574
Mean	1.09	0.47	0.62	78	6256372	585	144483

TABLE VII. EPR-MOGA SETTINGS USED IN THIS STUDY

Setting	Value used
Regression type	Static
Expression type	Y = Σ a_i · X1 · X2 · f(X1) · f(X2) + a_0
Inner function f(·)	No function
Number of terms searched	1 to 8 (final models: four terms plus a bias term)
Candidate exponents	[−2, −1, −0.5, 0, 0.5, 1.0, 2.0]
Bias term	Included
Coefficient estimation	Least squares (LS)
Number of generations	10
MOGA strategy (objectives)	Minimize the number of terms and the sum of squared errors, Min(aj, SSE)
Scaling of inputs and outputs	None

TABLE VIII. ACCURACY MEASURES OF EQUATION 9 (EQUIVALENT THICKNESS)

Accuracy measure	Training set	Testing set
MAE	97	100
Mean	1.0	1.0
R	0.86	0.84

TABLE IX. ACCURACY MEASURES OF EQUATION 10 (EQUIVALENT STIFFNESS)

Accuracy measure	Training set	Testing set
MAE	15612	18078
Mean	1.01	1.00
R	0.94	0.94

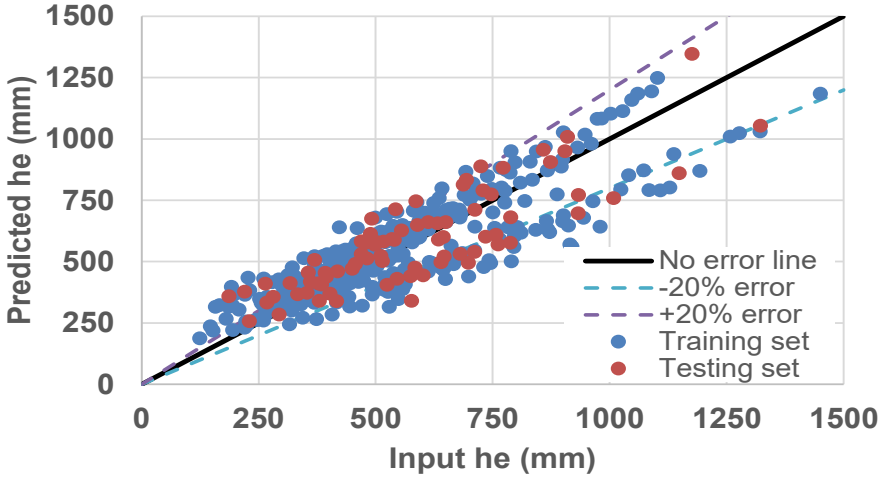


Fig. 6. Comparison of measured and predicted equivalent thickness of the pavement section for training and testing sets

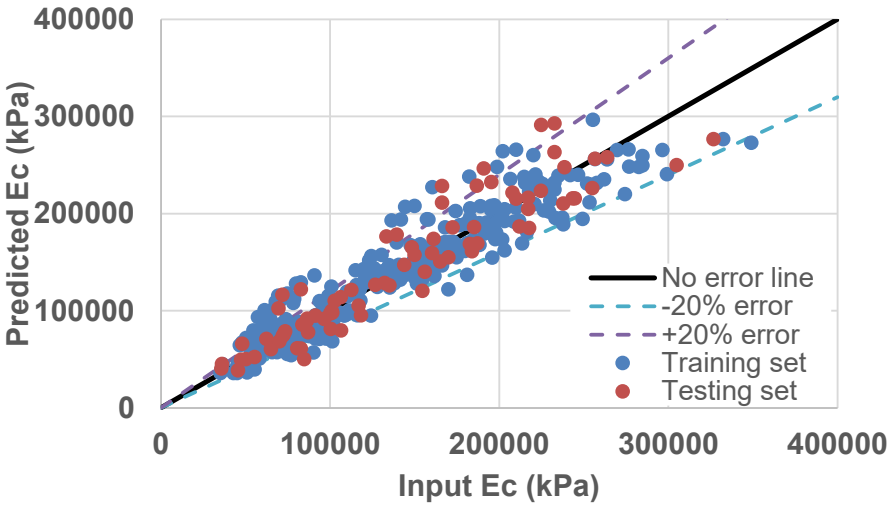


Fig. 7. Comparison of measured and predicted equivalent stiffness of the pavement section for training and testing sets

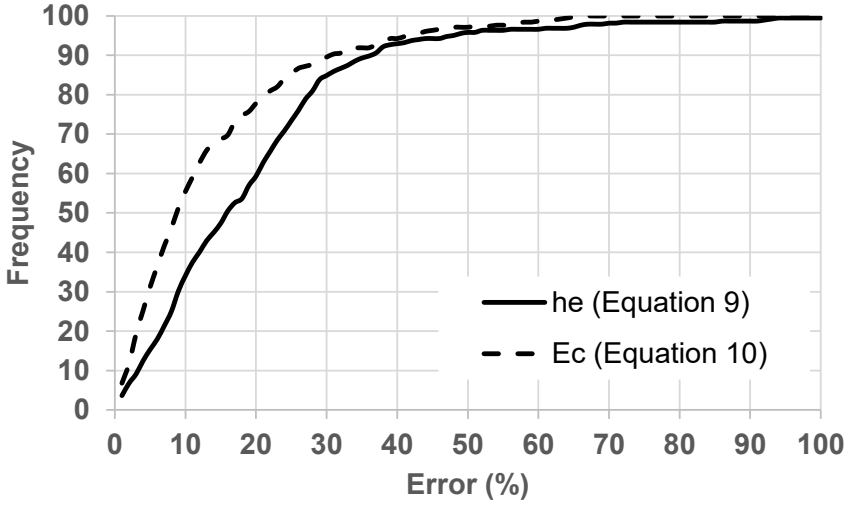


Fig. 8. Cumulative frequency of error of prediction for the equivalent thickness and equivalent stiffness

7. CONCLUSIONS

A validated finite element model has been developed to correctly replicate the results of the FWD test using the Plaxis 3D software package. The model is then utilized to develop a robust database of different scenarios of the FWD test to enable the development of new models that could be utilized for quick prediction of the equivalent thickness and stiffness of the pavement section using the multi-objective evolutionary polynomial regression analysis developed by Giustolisi and Savic [16]. The following conclusions could be stated based on the findings of this research study:

1. Plaxis 3D correctly replicated the FWD test.
2. The equation developed to predict the equivalent thickness scored reasonably well in the accuracy check, as it scored MAE, mean, and R values of 97, 1.00, and 0.86, respectively, for the training set and 100, 1.00, and 0.84 for the testing set.
3. The developed equation to estimate the equivalent stiffness also scored well in accuracy with values of MAE, mean, and R of 15612, 1.01, and 0.94, respectively, for the training set and 18078, 1.00, and 0.94, respectively, for the testing set.
4. The developed models of the equivalent thickness and equivalent stiffness require basic inputs that could be readily obtained from the FWD test and asphalt core sample. Thus, these models could be of significant usefulness to pavement engineers who work on the quality control of pavement sections.

Finally, it should be stressed that the proposed models are intended to provide practical tools for pavement evaluation within the range of conditions considered in this study, which are explicitly stated in Tables 2 and 4. The model's applicability is supported by the statistical performance obtained during the development and evaluation of the models, which are discussed in detail in Section 6 and explained in the aforementioned points. Also, the purpose of the models is to simplify the estimation of equivalent pavement thickness and stiffness from readily available FWD and pavement data, rather than to replace all existing back-calculation methods under every possible pavement condition. The authors consider the proposed models as useful alternatives for cases falling within their established applicability range, while recognizing that further evaluation may be beneficial when applying them to conditions beyond those investigated in this study.

Acknowledgement

None

Funding

The authors did not receive any funding for this research.

Conflicts of Interest

The authors declare no competing interests.

Ethical Approval

This study did not involve human or animal subjects, and ethical approval was not required.

Author Contributions

****Saif Alzabeebee**:** Conceptualization; Data curation; Formal analysis; Investigation; Methodology; Software; Validation; Visualization; Writing – original draft. ****Suraparb Keawsawasvong**:** Conceptualization, Methodology, Validation, Writing – review & editing.

Data Availability Statement

The database developed in this study is included as a supplementary material.

References

[1] E. Horak, “Application of equivalent-layer-thickness concept in a mechanistic rehabilitation design procedure,” Transportation Research Record, vol. 1207, pp. 69–75, 1988.

[2] S. Sharma and A. Das, “Backcalculation of pavement layer moduli from falling weight deflectometer data using an artificial neural network,” Canadian Journal of Civil Engineering, vol. 35, no. 1, pp. 57–66, 2008, doi: 10.1139/L07-083

[3] M. Saltan, V. E. Uz, and B. Aktas, “Artificial neural networks–based backcalculation of the structural properties of a typical flexible pavement,” Neural Computing and Applications, vol. 23, no. 6, pp. 1703–1710, 2013, doi: 10.1007/s00521-012-1131-y.

[4] S. Terzi, M. Saltan, E. U. Küçüksille, and M. Karaşahin, “Backcalculation of pavement layer thickness using data mining,” Neural Computing and Applications, vol. 23, no. 5, pp. 1369–1379, 2013, doi: 10.1007/s00521-012-1083-2.

[5] B. Phulsawat, A. Senjuntichai, and T. Senjuntichai, “Prediction of multi-layered pavement moduli based on falling weight deflectometer test using soft computing approaches,” Transportation Infrastructure Geotechnology, vol. 11, no. 4, pp. 1–34, 2024, doi: 10.1007/s40515-024-00370-1.

[6] X. Ma, C. Ren, X. Han, X. Li, S. Ullah, Z. Dong, W. Quan, T. Emmanuel, and K. Liu, “Multi-machine learning framework for the modulus back-calculation of asphalt pavement using measured FWD deflection basin,” Construction and Building Materials, vol. 538, Art. no. 147222, 2026, doi: 10.1016/j.conbuildmat.2026.147222.

[7] G. Wang and Y. Zhao, “Intelligent pavement moduli back-calculation using an SEM–transformer framework,” Frontiers in Materials, vol. 12, Art. no. 1732297, 2025, published online Jan. 28, 2026, doi: 10.3389/fmats.2025.1732297.

[8] Gajewski, Marcin Daniel, Pengyuan Xia, Beata Gajewska, Jorge Pais, and Mikołaj Miecznikowski. "Estimation of the XGBoost Regression Model Used in the Prediction of Pavement's Mechanical and Geometrical Parameters Based on Static Interpretation of the FWD Test." Applied Sciences 15, no. 24 (2025): 12943, https://doi.org/10.3390/app152412943.

[9] P. Ullidtz, Pavement Analysis. Amsterdam, The Netherlands: Elsevier, 1987.

[10] K. D. Smith, J. E. Bruinsma, M. J. Wade, K. Chatti, J. M. Vandenbossche, and H. T. Yu, "Using falling weight deflectometer data with mechanistic-empirical design and analysis, Volume I: Final report," FHWA-HRT-16-009, Federal Highway Administration, Mar. 2017.

[11] J. Lysmer and R. L. Kuhlemeyer, "Finite dynamic model for infinite media," Journal of the Engineering Mechanics Division, vol. 95, no. 4, pp. 859–877, 1969, doi: 10.1061/JMCEA3.0001144.

[12] Bentley Systems (2020) PLAXIS CONNECT Edition V20.04: Scientific Manual. Delft: Bentley Systems. Available at: PLAXIS Scientific Manual V20.04 (Accessed: 18 July 2026).

[13] M. M. Tawfik and Y. M. El-Mossallamy, "Application of the finite element method for investigating the dynamic plate loading test," Ain Shams Engineering Journal, vol. 8, no. 1, pp. 39–49, 2017, doi: 10.1016/j.asej.2015.08.011.

[14] A. Hamim, N. I. M. Yusoff, H. Ceylan, S. A. P. Rosyidi, and A. El-Shafie, "Comparative study on using static and dynamic finite element models to develop FWD measurement on flexible pavement structures," Construction and Building Materials, vol. 176, pp. 583–592, 2018, doi: 10.1016/j.conbuildmat.2018.05.082.

[15] S. Fathi, M. Mehravar, and M. Rahman, "Development of FWD based hybrid back-analysis technique for railway track condition assessment," Transportation Geotechnics, vol. 38, Art. no. 100894, 2023, doi: 10.1016/j.trgeo.2022.100894.

[16] S. Fathi, M. Mehravar, and M. Rahman, "A hybrid artificial neural network–genetic algorithm back-analysis technique for local anomaly detection in railway track substructure," Proceedings of the Institution of Civil Engineers—Transport, vol. 178, no. 6, pp. 375–392, 2025, doi: 10.1680/jtran.23.00066.

[17] A. Loizos and A. Scarpas, "Verification of falling weight deflectometer backanalysis using a dynamic finite elements simulation," International Journal of Pavement Engineering, vol. 6, no. 2, pp. 115–123, 2005, doi: 10.1080/10298430500141030.

[18] O. Giustolisi and D. A. Savic, "Advances in data-driven analyses and modelling using EPR-MOGA," Journal of Hydroinformatics, vol. 11, nos. 3–4, pp. 225–236, 2009, doi: 10.2166/hydro.2009.017.

[19] A. Ahangar-Asr, A. Johari, and A. A. Javadi, "An evolutionary approach to modelling the soil–water characteristic curve in unsaturated soils," Computers & Geosciences, vol. 43, pp. 25–33, 2012, doi: 10.1016/j.cageo.2012.02.021.

[20] B. O. da Silva and G. J. C. Gomes, "Evolutionary polynomial regression (EPR) applications in geotechnical engineering: A comprehensive survey, uncertainty analysis, and physical interpretation of models," Arabian Journal of Geosciences, vol. 19, Art. no. 76, 2026, doi: 10.1007/s12517-026-12459-7.

[21] S. Alzabeebee, "Application of EPR-MOGA in computing the liquefaction-induced settlement of a building subjected to seismic shake," Engineering with Computers, vol. 38, Suppl. 1, pp. 437–448, 2022.

[22] C. Ye, X. Chen, and H. Sun, "Weak physics-informed neural network prediction of excavation-induced longitudinal heave in existing shield tunnels," Transportation Infrastructure Geotechnology, vol. 13, Art. no. 239, 2026, doi: 10.1007/s40515-026-01009-z.

[23] D. Padmini, K. Ilamparuthi, and K. P. Sudheer, "Ultimate bearing capacity prediction of shallow foundations on cohesionless soils using neurofuzzy models," Computers and Geotechnics, vol. 35, no. 1, pp. 33–46, 2008, doi: 10.1016/j.compgeo.2007.03.001.

[24] O. I. Selezneva, Y. J. Jiang, and G. Mladenovic, "Evaluation and analysis of LTPP pavement layer thickness data," FHWA-RD-03-041, Federal Highway Administration, Washington, DC, USA, 2002.

[25] P. N. N. Nogima, J. Yu, S. C. J. Moya, Z. Yang, and Y. Lin, "Performance-based optimization of asphalt mixtures for tropical pavement structures: A mechanistic and fatigue life approach," Buildings, vol. 16, no. 15, Art. no. 3004, 2026, doi: 10.3390/buildings16153004.

[26] B. R. Christopher, C. Schwartz, and R. Boudreau, *Geotechnical Aspects of Pavements*, FHWA-NHI-05-037. Washington, DC, USA: Federal Highway Administration, May 2006.

[27] Ministry of Transport of the People's Republic of China, Specifications for Design of Highway Asphalt Pavement (JTG D50–2017). Beijing, China: Ministry of Transport of the People's Republic of China, 2017.

[28] P. Li, M. Zheng, F. Wang, F. Che, H. Li, Q. Ma, and Y. Wang, "Laboratory performance evaluation of high modulus asphalt concrete modified with different additives," Advances in Materials Science and Engineering, vol. 2017, Art. no. 7236153, 2017, doi: 10.1155/2017/7236153.

[29] D. Nguyen, T. K. Le, and T. C. Do, "Influence of asphalt concrete thickness on rutting performance of full-depth flexible pavement based on modulus-derived analysis," in Hydraulic and Civil Engineering Technology X: Proc. 10th Int. Technical Conf., vol. X, 2026, pp. 506–512, doi: 10.3233/ATDE251268.

[30] J. Yi, C. Liang, J. Qian, J. Li, and Y. Yao, "Laboratory evaluation and design of construction and demolition wastes for granular base," Advances in Civil Engineering, vol. 2020, Art. no. 8827715, 2020, doi: 10.1155/2020/8827715.

[31] B. T. Chua, H. Abuel-Naga, and K. P. Nepal, "Design charts for geogrid-reinforced granular working platform for heavy tracked plants over clay subgrade," Transportation Infrastructure Geotechnology, vol. 10, pp. 795–815, 2023, doi: 10.1007/s40515-022-00243-5.

[32] L. M. Pierce, J. E. Bruinsma, K. D. Smith, M. J. Wade, K. Chatti, and J. M. Vandenbossche, "Using falling weight deflectometer data with mechanistic-empirical design and analysis, Volume III: Guidelines for deflection testing, analysis, and interpretation," FHWA-HRT-16-011, Federal Highway Administration, Dec. 2017.

[33] A. M. Alani and A. Faramarzi, "An evolutionary approach to modelling concrete degradation due to sulphuric acid attack," Applied Soft Computing, vol. 24, pp. 985–993, 2014, doi: 10.1016/j.asoc.2014.08.044.

[34] A. M. Alani, A. Faramarzi, M. Mahmoodian, and K. F. Tee, "Prediction of sulphide build-up in filled sewer pipes," Environmental Technology, vol. 35, no. 14, pp. 1721–1728, 2014, doi: 10.1080/09593330.2014.881403.